Electronic band structure of isotopically pure germanium: Modulated transmission and reflectivity study

C. Parks, A. K. Ramdas, and S. Rodriguez
Department of Physics, Purdue University, West Lafayette, Indiana 47907

K. M. Itoh and E. E. Haller
Lawrence Berkeley Laboratory and University of California at Berkeley, Berkeley, California 94720
(Received 24 January 1994)

The piezomodulated and photomodulated reflectivity spectra of monoisotopic Ge (^{70}Ge, ^{73}Ge, ^{74}Ge, ^{76}Ge) and natural Ge measured at $T = 6$ K show clear signatures of the E_0 and the $E_0 + \Delta_0$ transitions; their energies increase with increasing isotopic mass. From a comparison of the phonon-assisted indirect transition energies obtained from electromodulated and wavelength-modulated transmission and photoluminescence, the isotopic mass dependence of both the indirect gap and the relevant zone-boundary phonons are deduced. The isotopic-mass dependence of the energy gaps are interpreted in the context of the electron-phonon interaction and the volume expansion of the crystal lattice.

I. INTRODUCTION

The electronic band structure of semiconductors shows a temperature and pressure dependence which can be most readily observed in the optical transitions between the critical points of the Brillouin zone (BZ). In the first observation on the indirect transitions between the Γ_8^+ valence band maximum and the absolute conduction band minima at L_6^+ (Δ_6) for Ge (Si), Becker and Fan reported that the absorption edge in Ge and Si shift to higher energies as the temperature is lowered.[1] Both the temperature dependence and the pressure dependence of the energy gaps at various points within the BZ deduced from experimental observations have been documented in the literature.[2]

In light of the physical mechanisms underlying the temperature dependence of the energy gaps, it is important to take into account the isotopic composition of a given semiconductor. At low temperature, the isotopic shift of the energy gap should vary as $M^{-1/2}$, where M is the average isotopic mass of the constituent atoms. For a complete theoretical description of temperature and isotopic effects in group-IV semiconductors see Refs. 3–10.

Among the group-IV elemental semiconductors (C, Si, Ge, and Sn) Ge has a wide range of stable isotopes spanning ^{70}Ge to ^{76}Ge, second only to that of Sn.[11] In recent years, single crystals of monoisotopic Ge have been grown using isotopes separated by gas centrifuge, thus creating the opportunity for many basic studies.[12] Raman scattering has yielded phonon energies at the zone center[13,14] and at several critical points of the BZ.[14] In addition, experimental observations on the isotopic disorder-induced Raman scattering have been reported.[14,15] Photoluminescence at the indirect gap provides the isotopic shift of the Γ_8^+-L_6^+ transition energies as well as those of the zone-boundary phonons involved in the indirect optical transition.[13,16–18] Ellipsometric studies of the isotopic dependence of the E_1 and $E_1 + \Delta_1$ direct gaps have also been reported.[9] The isotopic dependence of E_0 has only been previously reported on very thin specimens of natural Ge and ^{76}Ge by a transmission measurement.[13]

In the present paper the focus is on the exploration and delineation of the isotopic dependence of the direct energy gaps (E_0, E_1, $E_0+\Delta_0$, and $E_1+\Delta_1$) by exploiting the advantages of modulation spectroscopy[19] with photomodulated and piezomodulated reflectivity. In addition, the piezomodulated, electromodulated, and wavelength-modulated transmission spectra reported in this paper reveal clearly the indirect gap and its phonon-assisted transitions including the structure associated with the mass anisotropy of the conduction band minima.[20–22] Modulation spectroscopy is particularly well suited for measuring the direct gaps since it is does not entail loss of material when samples are prepared with micrometer scale thicknesses needed for transmission measurements. (This is particularly important in view of the extremely high value of isotopically pure materials.) In order to deduce the values of the indirect gap and the associated phonon energies we also performed photoluminescence experiments.

II. EXPERIMENT

Isotopically enriched germanium single crystals were grown using the vertical Bridgman technique with a programmed temperature ramp. The crucible material was graphite and the ambient, nitrogen. A detailed description of our growth technique has been given in Ref. 12. The isotopic composition of each sample determined by secondary ion mass spectrometry is given in Table I. In

TABLE I. The percentage isotopic composition of the specimens studied. The accuracy of the isotopic composition of the enriched specimens is ±0.1%. All masses are in amu.

Nominal	Isotope mass (amu)					
isotope	69.924	71.922	72.923	73.922	75.921	Average
Natural[a]	21.23	27.66	7.73	35.94	7.44	72.59
^{70}Ge	96.3	3.7				70.00
^{73}Ge		2.0	95.6	2.4		72.93
^{74}Ge	0.5	0.1	2.2	96.8	0.4	73.89
^{76}Ge				13.5	86.5	75.65

[a]Reference 23.

the rest of the paper we identify the samples by their nominal isotope label.

All samples measured had typical thicknesses in the range 0.7–1.5 mm. They were first polished with a 3 μm diamond paste followed by a 0.05 μm Syton[24] polish-etch solution immediately before the reflectivity measurements.

The E_0 and $E_0 + \Delta_0$ direct energy gaps of the germanium isotopes were measured by photomodulated reflectivity, the modulating laser radiation being the 5145 Å line of an Ar^+ laser chopped at 498 Hz. The sample was illuminated with a typical power density of 2 mW/cm^2 and a 8000 Å long-pass filter was used to eliminate stray laser radiation from reaching a Ge photodiode at 300 K used as the detector.

The Γ_8^+-L_6^+ indirect energy gap was measured by photoluminescence, electromodulated, piezomodulated, and wavelength-modulated transmission. For piezomodulated transmission the samples were attached with Apiezon N grease to the end of a lead-zirconate-titanate transducer in the form of a cylinder 6 mm long with inner and outer diameters of 5 mm and 10 mm, respectively. The radial expansion and contraction of the cylinder driven by an ac voltage of 560 V rms produced an alternating strain in the sample. Light from the monochromator passed through the sample along the axis of the cylinder. The wavelength modulation was achieved by mounting a 6 mm thick glass plate[25] on a motor shaft in front of the monochromator exit slit. The plate was tilted 1.5° off normal to the motor shaft and rotated at 42 Hz. Electromodulated transmission was accomplished in a manner similar to that used in electromodulated reflectivity.[26] The sample was placed between two flat copper plates separated by 2 mm with a 10 × 0.5 mm wide slit in the center of each plate. The sample was placed between the plates and electrically insulated from each plate by a thin glass slide. Light was transmitted through the slit in each plate and the sample while an ac voltage of 650 V rms was applied on the plates. All the photomodulation, electromodulation, and piezomodulation measurements employed a Janis SuperTran[27] optical cryostat to cool the samples to 6 K. Wavelength-modulation measurements required the use of a glass optical cold finger cryostat with wedged glass windows in order to eliminate interference fringes associated with cryostat windows. The light source consisted of a 600 W tungsten halogen lamp. The monochromator used for electromodulation, photomodulation, and piezomodulation was a Perkin-Elmer (model $E1$) double-pass grating monochromator while wavelength-modulation experiments were carried out with a Spex 1402 double grating monochromator. A Ge photodiode at 300 K was used for measurements on the indirect and direct gaps below 1.2 eV. A Si photodiode was used for the E_1 and $E_1 + \Delta_1$ energy gaps above 1.2 eV. The modulated components of the reflectivity ΔR or transmission ΔT and the unmodulated components R or T were measured simultaneously in order to obtain the ratios $\Delta R/R$ or $\Delta T/T$. The operation of the monochromators and collection of the data were carried out with a microcomputer. Photoluminescence measurements were performed at 6 K using the 5145 Å Ar^+ laser line for excitation with a typical power density was 50 mW/mm^2. The luminescence was spectrally analyzed with a Perkin-Elmer (model $E1$) spectrometer and detected with a Ge photodiode at 300 K.

III. THEORETICAL CONSIDERATIONS

The energy gaps in the electronic energy bands of a semiconductor vary with temperature as a consequence of the electron-phonon interaction on the one hand and the thermal expansion on the other hand. The temperature differential coefficient of an energy gap E_g at constant pressure can be expressed as

$$\left(\frac{\partial E_g}{\partial T}\right)_P = \left(\frac{\partial E_g}{\partial T}\right)_V - \beta B \left(\frac{\partial E_g}{\partial P}\right)_T , \qquad (1)$$

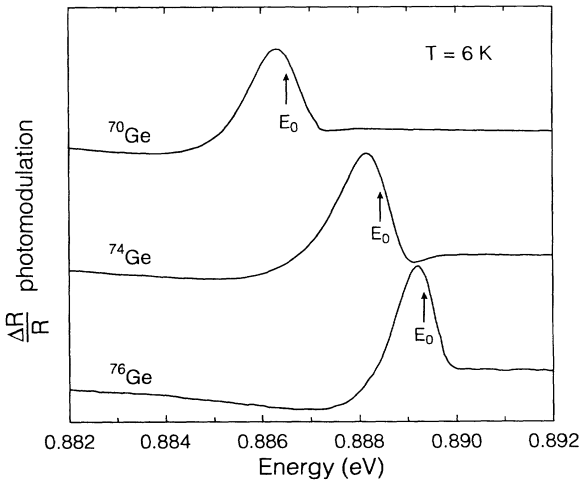

FIG. 1. Photomodulated reflectivity showing the E_0 direct gap of single crystals of ^{70}Ge, ^{74}Ge, and ^{76}Ge at $T = 6$ K.

where $\beta = (1/V)(\partial V/\partial T)_P$ is the coefficient of volume thermal expansion, and B is the isothermal bulk modulus. Two contributions called *self-energy*[4] and *Debye-Waller*[5] terms have been identified as the microscopic mechanisms underlying the pure temperature coefficient $(\partial E_g/\partial T)_V$.

The change in energy of an electronic state due to the electron-phonon coupling results from the first order interaction taken in second order perturbation theory and the quadratic interaction taken in first order. The former is called the self-energy and the latter, the Debye-Waller term. Both terms involve expressions quadratic in atomic displacements characterized by $u_{\mathbf{n}}(\mathbf{q}, j)$, where $\mathbf{n}$ denotes the lattice site, $\mathbf{q}$ the wave vector of a phonon belonging to branch j, with the corresponding thermal averages $\langle u^2_{\mathbf{n}}(\mathbf{q}, j)\rangle = (\hbar/M\omega_{\mathbf{q}j})(\overline{n}_{\mathbf{q}j} + \frac{1}{2})$, $\overline{n}_{\mathbf{q}j}$ being the associated Bose-Einstein occupation number, and M the average atomic mass. (The use of the average mass is implicit in the virtual crystal approximation in the lattice dynamics of crystals with random isotopic disorder.) A comprehensive discussion and theoretical estimates of the terms in Eq. (1) have been presented in Refs. 6–8. In the present paper the focus is on effects associated with the isotopic constitution of the crystal. At $T = 0$ K, the difference in an energy gap E_g between crystals having average atomic masses M and $M + \Delta M$ can be expressed as

$$\Delta E_g = \left[\left(\frac{\partial E_g}{\partial M}\right)_{T,V} - B\left(\frac{\partial E_g}{\partial P}\right)_T \frac{1}{V}\left(\frac{\partial V}{\partial M}\right)_{P,T}\right]\Delta M. \tag{2}$$

The first term in Eq. (2) results from the superposition of the self-energy and Debye-Waller terms already discussed. At $T = 0$ K, the mean square displacement $\langle u^2_{\mathbf{n}}(\mathbf{q}, j)\rangle$ becomes proportional to $(\hbar/2M\omega_{\mathbf{q}j})$, arising from the zero-point contribution. Thus, the self-energy and Debye-Waller terms are both proportional to $M^{-\frac{1}{2}}$ under the assumption that the phonon frequencies scale as the inverse square root of the isotopic mass. However, we note that at high temperatures $\langle u^2_{\mathbf{n}}(\mathbf{q}, j)\rangle \approx (kT/M\omega^2_{\mathbf{q}j})$ becomes independent of M and the isotopic effects should progressively become less important with increasing temperature. The second term in Eq. (2) arises from the difference between the atomic volumes of the two crystals with isotopic masses M and $M + \Delta M$, which according to Buschert *et al.*[28] is given by

$$\frac{\Delta V}{V} = -\frac{\Delta M}{4BMV}\sum_{\mathbf{q}j}\hbar\omega_{\mathbf{q}j}\gamma_{\mathbf{q}j}, \tag{3}$$

where $\gamma_{\mathbf{q}j} = -\partial(\ln\omega_{\mathbf{q}j})/\partial(\ln V)$, the Grüneisen parameter associated with the mode $\mathbf{q}j$. Equation (3) implies that $V - V^\infty$ is proportional to $M^{-\frac{1}{2}}$, where V^∞ is the volume in the limit of infinite isotopic mass. (The γ's are expected to vary linearly with M.)

In Refs. 6–9 the self-energy and Debye-Waller terms were obtained at 0 K as well as at finite temperature. Here we focus on the low temperature limits. We conclude that both contributions in Eq. (2) vary as $M^{-\frac{1}{2}}$ and, thus, cannot be separated without measuring the lattice parameters for each isotope which, in turn, yields $(1/V)(\partial V/\partial M)_{P,T}$. As it will be shown in the next section, the contribution of the change in lattice constant is a significant fraction of ΔE_g.

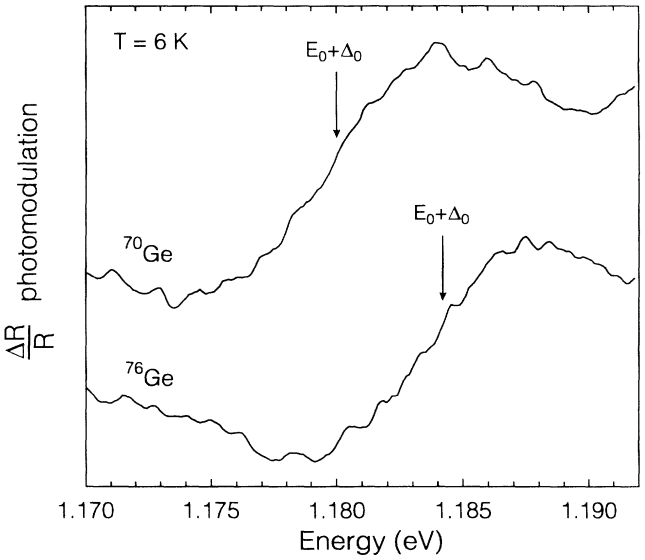

FIG. 2. Photomodulated reflectivity spectra of the $E_0 + \Delta_0$ direct gap of ^{76}Ge and ^{70}Ge at $T = 6$ K.

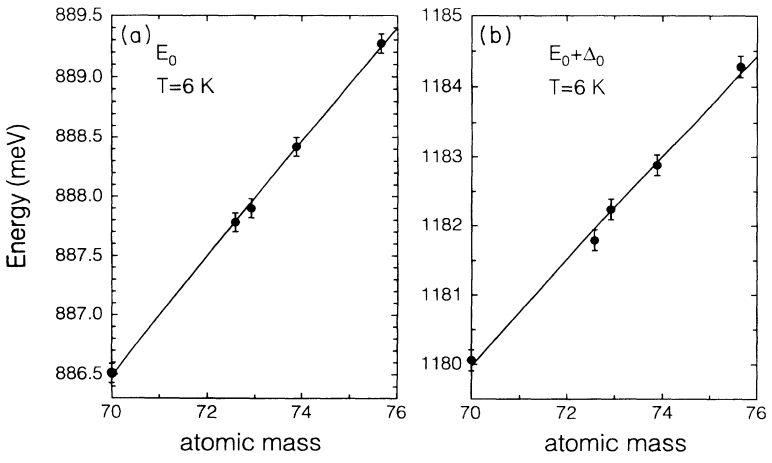

FIG. 3. Isotopic mass (in amu) dependence of the (a) E_0 and (b) $E_0 + \Delta_0$ direct energy gaps obtained from photomodulated reflectivity measurements at $T = 6$ K. The curves are the best fit to Eq. (4).

IV. RESULTS AND DISCUSSION

A. Direct gaps

Figure 1 shows the photomodulated reflectivity spectra of ^{70}Ge, ^{74}Ge, and ^{76}Ge in the energy range of E_0, the lowest direct gap at the BZ center corresponding to the Γ_8^+-Γ_7^- optical transitions. The large signal strength enabled the spectra to be recorded with an excellent signal to noise ratio. The values of E_0 in the photomodulated spectra, were obtained by fitting the spectra to the third derivative of a Lorentzian exciton line shape.[29] No significance is attached to the small variations in the line shapes between the spectra for the different isotopes because they depend, to some extent, on the quality of the sample surface as well as on the modulating laser wavelength employed. They clearly show the isotopic dependence of E_0.

The mass dependence of E_0 was fitted with the function

$$E_0 = E_0^{\infty} + \frac{C}{\sqrt{M}}, \tag{4}$$

where M is the atomic mass and E_0^{∞} is the energy gap at $M = \infty$. The fitting yields $E_0^{\infty} = 959$ meV and $C = -606$ meV amu$^{1/2}$. Over the small range of isotopic masses available for Ge, the mass dependence in Eq. (4) can be approximated by a linear fit, yielding $(\partial E_0/\partial M) = 0.49$ meV/amu.

The $E_0 + \Delta_0$ transitions shown in Fig. 2 for photomodulation are significantly weaker than the E_0 transitions. However, the isotopic shift is still discernable. Following the curve fitting procedure used for E_0, the linear shift in $E_0 + \Delta_0$ was determined to be 0.74 meV/amu. Combining this with the results of the E_0 measurements, the isotopic dependence of the spin-orbit splitting is therefore 0.25 meV/amu. Figure 3 displays the isotopic mass dependence of E_0 and $E_0 + \Delta_0$.

Figure 4 shows the piezomodulated reflectivity spectra of the E_1 and $E_1 + \Delta_1$ transitions for ^{76}Ge and ^{70}Ge. The very large natural width of these transitions prevented a reliable determination of their isotopic shifts.

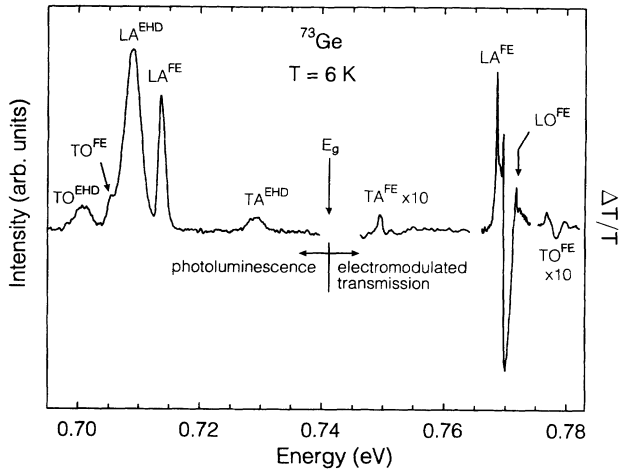

FIG. 5. Photoluminescence and electromodulated transmission spectra of ^{73}Ge. The intensity scales are arbitrary and are not corrected for the spectral response of the detector. Both spectra were recorded at $T = 6$ K.

B. Indirect gap

Since the Γ_8^+-L_6^+ optical transition is indirect, phonon emission or absorption must accompany the electronic transition in order to ensure conservation of crystal momentum. The relevant phonons (the longitudinal and transverse acoustic, LA and TA, as well as the longitudinal and transverse optic, LO and TO) are those with wave vectors at the L point in the BZ. At low temperatures, in the absorption process associated with the indirect transition (detected in modulated transmission),

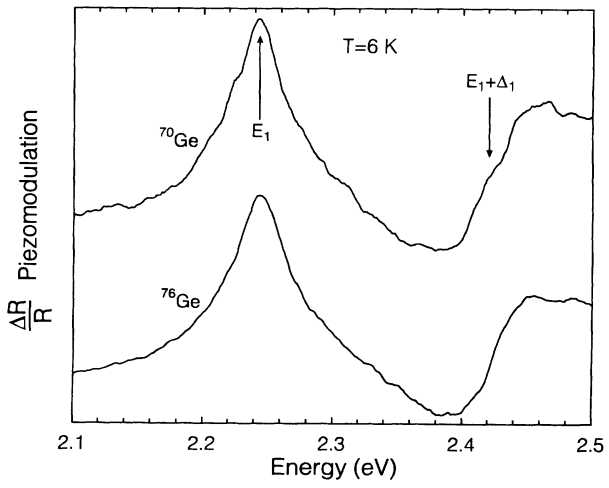

FIG. 4. Piezomodulated reflectivity spectra of the E_1 and $E_1 + \Delta_1$ direct gaps of ^{76}Ge and ^{70}Ge at $T = 6$ K.

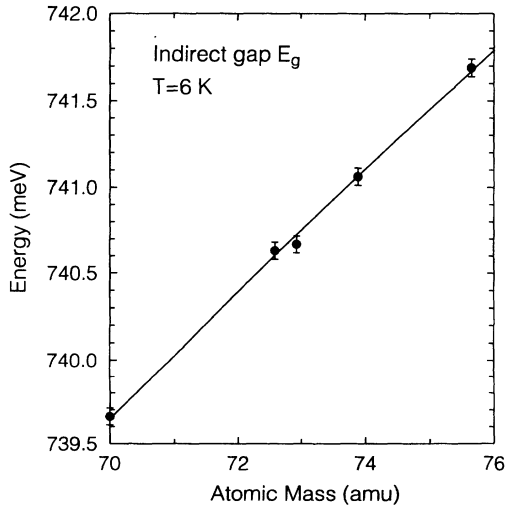

FIG. 6. Atomic mass dependence of the indirect gap E_g at $T = 6$ K.

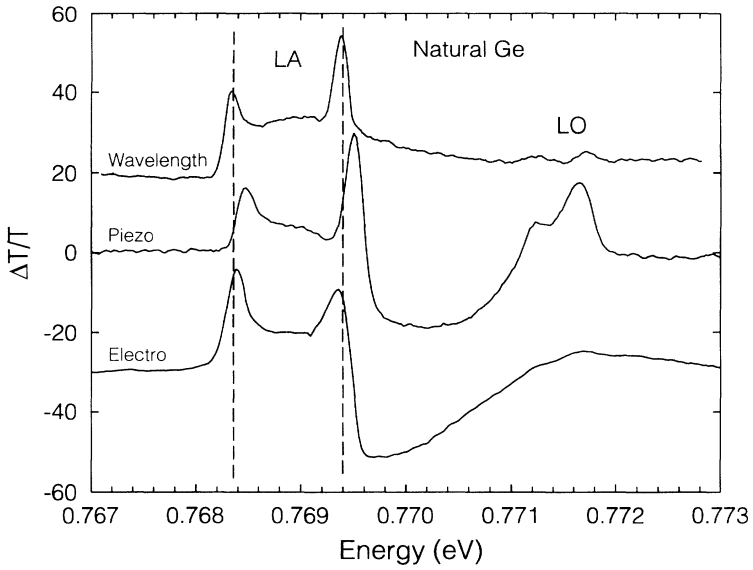

FIG. 7. Electromodulated, piezomodulated, and wavelength-modulated transmission spectra of the LA and LO phonon-assisted indirect optical transitions of natural Ge at $T = 6$ K. The vertical dashed lines indicate the energies of the LA phonon doublet features in electromodulated and wavelength-modulated transmission. The piezomodulation spectrum is shifted by ≈ 0.1 meV due to strain induced by differential thermal contraction.

the spectral features occur at the energy gap E_g, *plus* one phonon energy $\hbar\omega_{\rm ph}$. On the other hand, in photoluminescence, spectral features appear at the energy gap *minus* one phonon energy. Hence, E_g is the average of the indirect transition energies observed in absorption and photoluminescence whereas their difference is $2\hbar\omega_{\rm ph}$. Thus, it is possible to combine the results of photoluminescence and modulated transmission to deduce the isotopic dependence of both E_g and $\hbar\omega_{\rm ph}$.

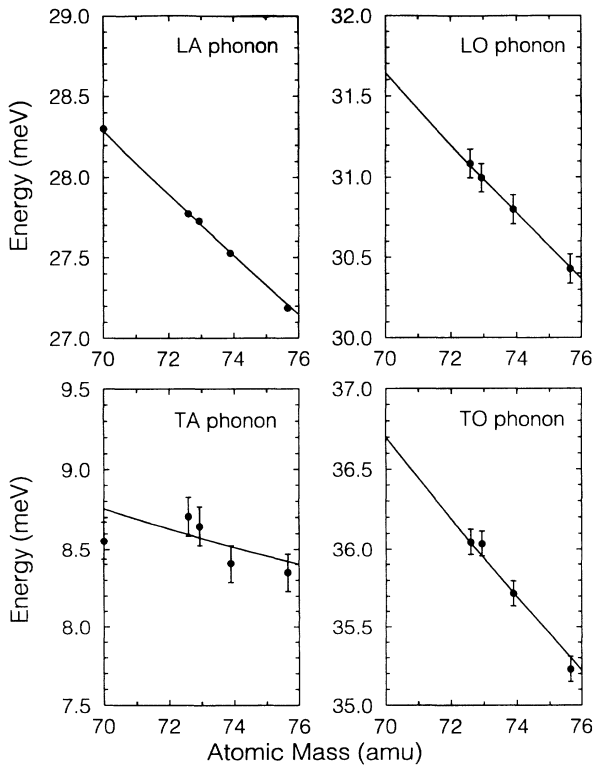

FIG. 8. The LA, LO, TA, and TO phonon energies of the L point of Ge as a function of atomic mass at $T = 6$ K. The fitted curves are a one parameter fit to Eq. (5).

Figure 5 shows the spectra for ^{73}Ge obtained by photoluminescence for energies less than E_g and electromodulated transmission for energies greater than E_g. The power density of the photoluminescence exciting laser was high enough to allow the observation of features associated with both the free exciton and the electron hole droplet (EHD). The photoluminescence of the LA and TO free exciton energies were determined from data recorded at lower power densities in order to eliminate the EHD feature. For all the Ge isotopes the photoluminescence revealed signatures at the LA and TO phonon energies while the electromodulated transmission measurements revealed signatures for all four phonons. Figure 6 shows the variation of E_g as a function of atomic mass yielding $(\partial E_g/\partial M)$ to be 0.36 meV/amu.

Figure 7 shows the electro-modulated, piezomodulated, and wavelength-modulated transmission spectra of the LA and LO phonon-assisted indirect optical transitions. We note that the LA phonon feature is a doublet as a result of the splitting of the $1s$ exciton state arising from the anisotropy of the L_6^+ conduction band minimum.[20–22] An exact line fitting of the LA phonon peaks is not possible because of the mass reversal effect.[30] The isotopic shift of the two LA phonon peaks was determined from the energy of the same spectral feature on each LA phonon-assisted peak for each Ge sample. From the shifts of the LA phonon peak and that of E_g, we de-

TABLE II. Isotope shifts of the energies of the interband optical transitions between the critical points of the electronic band structure of Ge as well as the fitted parameters E^{∞} and C of Eq. (4). All values are at $T = 6$ K.

Transition	Shift (meV/amu)	E^{∞} (meV)	C (meV amu$^{\frac{1}{2}}$)
E_g	0.36	793± 2	−445± 12
E_0	0.49	959± 2	−606± 11
$E_0 + \Delta_0$	0.74	1291± 5	−926± 39
Δ_0	0.25	332± 7	−319± 50

duce a shift of -0.19 meV/amu for the LA phonon. In a similar manner we obtain the shift of the LO phonon as -0.21 meV/amu. The present measurements yield the splitting of the two LA phonon $1s$ exciton peaks to be 1.11 ± 0.03 meV. We did not observe any measurable isotopic dependence of the $1s$ exciton splitting.

A comparison of the three modulation techniques in Fig. 7 shows that the piezomodulation spectral features occur ≈ 0.1 meV higher in energy than those observed in wavelength modulation or electromodulation. This is attributed to a small strain induced by the differential thermal contraction between the Ge sample and the piezoelectric transducer to which it was fixed. The origin of the dip in the piezomodulated and electromodulated spectra between the LA and LO phonon features is not clear and was not observed in any of the wavelength-modulated spectra.

The electromodulated transmission measurements also revealed isotopic shifts in the energies of the TA and TO phonon-assisted transitions with $(\partial\hbar\omega_{\rm ph}/\partial M) = -0.059$ meV/amu and -0.25 meV/amu, respectively. The isotope shift of the phonon energies as a function of atomic mass measured by electromodulated transmission are displayed in Fig. 8. The curves in Fig. 8 are fitted according to

$$\hbar\omega_{\rm ph} = \frac{D}{\sqrt{M}}, \tag{5}$$

where D is the only adjustable parameter of the fit.

C. Discussion

We summarize the relevant quantitative features of the isotopic mass dependence of the electronic transitions in Table II and for the phonon energies in Table III. For the sake of completeness we remeasured the isotopic mass dependence of the zone center optical phonon (labeled Γ in Table III) as observed in the first order Raman spectrum; the results are consistent with those reported in Fuchs *et al.*[14] and Cardona *et al.*[31]

As noted in Sec III, the isotopic mass dependence of the energy gaps vary as $M^{-\frac{1}{2}}$ and the two terms in Eq. (2) corresponding to the electron-phonon interaction on the one hand and that due to the change in volume on the other, cannot be experimentally separated in the absence of lattice parameter measurements

TABLE III. Isotope shifts and the fitted parameter D of Eq. (5) for the Γ- and L-point phonons of Ge. All values are at $T = 6$ K.

Phonon	Shift (meV/amu)	D (meV amu$^{\frac{1}{2}}$)
TA (L)	-0.06	72.9 ± 1.4
LA (L)	-0.19	236.7 ± 0.4
LO (L)	-0.21	264.7 ± 0.8
TO (L)	-0.25	307.1 ± 0.9
Raman (Γ)	-0.26	320.9 ± 0.3

for *all* the isotopes. However, the values are available for natural Ge and ^{74}Ge in Buschert *et al.*[28] These authors have determined the relative change in lattice parameter at 78 K to be $(-14.9 \pm 0.3) \times 10^{-6}$ yielding $V^{-1}(\partial V/\partial M) = -3.29 \times 10^{-5}$ per amu.[32] Using the appropriate measured hydrostatic deformation potential constants, one can deduce the second term in Eq. (2), i.e., $(\Delta E_g/\Delta M)_{\rm vol}$, by multiplying the deformation potential by 3.29×10^{-5} amu^{-1}. The electron-phonon contributions, of course, are deduced from the experimentally measured isotopic shifts by subtracting the volume contribution. In Table IV we summarize the data by displaying the differential rates of change of E_0, $E_0+\Delta_0$, and the indirect gap E_g, including a comparison with the theoretical calculations of Zollner, Cardona, and Gopalan.[9] We note that the theory accounts for the isotopic mass behavior of E_g more satisfactorily than it does for E_0.

V. CONCLUDING REMARKS

In the present investigation a combination of modulation techniques and photoluminescence has been applied to the study of interband transitions of a number of monoisotopic Ge single crystals. The isotopic mass dependence of the energies of E_0 and $E_0+\Delta_0$ as well as that of E_g and the associated phonons have been delineated from these measurements.

Davies *et al.*[16] have reported the isotopic mass dependence of the indirect gap deduced from bound exciton transitions occurring in photoluminescence. In the "zero-phonon" bound excitonic indirect transitions, the isotopic mass dependence of the indirect gap can be established provided the excitonic binding energy is the same in all the isotopes. $(\partial E_g/\partial M) = 0.36$ meV/amu obtained in the present work is in excellent agreement with 0.35

TABLE IV. Linear isotope shifts of E_g, E_0, and $E_0 + \Delta_0$. The volume contribution is calculated from the deformation potential and the measured isotopic dependence of the lattice constant (Ref. 28). The deformation potential is in meV and the shifts are in meV/amu.

Transition	Deformation potential	$\left(\frac{\partial E}{\partial M}\right)$	$\left(\frac{\partial E}{\partial M}\right)_{\rm vol}$	$\left(\frac{\partial E}{\partial M}\right)_{\rm e\text{-}ph}$	$\left(\frac{\partial E}{\partial M}\right)_{\rm e\text{-}ph}$ (theory)
E_g	3800[a]	0.36	0.13	0.23	0.39[b]
E_0	10 900[c]	0.49	0.36	0.13	0.42[b]
$E_0 + \Delta_0$	11 200[c]	0.74	0.37	0.37	

[a]Reference 33.
[b]Theoretical result from Ref. 9.
[c]Reference 34.

meV/amu in Davies *et al.*[16] and in Etchegoin *et al.*[17] From the observation of phonon-assisted free excitonic features as well as the phonon sidebands of the bound excitonic transitions, the isotopic mass dependence of the TA, LA, and TO phonons at the L point were obtained by measuring their positions relative to the zero-phonon lines, assuming again that the excitonic binding energy is independent of the isotopic mass. The $\partial(\hbar\omega_{\rm ph}/\partial M)$ characterizing the data displayed in Ref. 17 and Fig. 2 of Ref. 18 are in very good agreement with our values listed in Table III. The analysis of the data obtained in the present investigations in the context of Eq. (2) underscores the importance of lattice parameter measurements for all the Ge isotopes at low temperatures.

ACKNOWLEDGMENTS

The work reported here has been supported in part by a grant from the National Science Foundation (Grant No. DMR-91-15856), at the University of California at Berkeley, and DOE (Grant No. DE-ACO3-76SF0098) at Lawrence Berkeley Laboratory, and by a grant from the National Science Foundation (Grant No. DMR-93-03186) at Purdue University.

[1] M. Becker and H. Y. Fan, Phys. Rev. **76**, 1530 (1949); **76**, 1531 (1949).
[2] *Semiconductors Group IV Elements and III-V Compounds*, edited by O. Madelung (Springer-Verlag, Heidelberg, 1991); *Semiconductors Other than Group IV Elements and III-V Compounds*, edited by O. Madelung (Springer-Verlag, Heidelberg, 1992).
[3] H. Y. Fan, Rep. Prog. Phys. **19**, 107 (1956).
[4] H. Y. Fan, Phys. Rev. **82**, 900 (1951).
[5] E. Antoncik, Czech. J. Phys. **5**, 449 (1955).
[6] P. B. Allen and M. Cardona, Phys. Rev. B **23**, 1495 (1981).
[7] P. B. Allen and M. Cardona, Phys. Rev. B **27**, 4760 (1983).
[8] P. Lautenschlager, P. B. Allen, and M. Cardona, Phys. Rev. B **31**, 2163 (1985).
[9] S. Zollner, M. Cardona, and S. Gopalan, Phys. Rev. B **45**, 3376 (1992). See also P. Etchegoin, H. D. Fuchs, J. Weber, M. Cardona, L. Pintschovius, N. Pyka, K. Itoh, and E. E. Haller, Phys. Rev. B **48**, 12 661 (1993), in particular Fig. 13.
[10] M. Cardona and S. Gopalan, *Progress on Electron Properties of Solids*, edited by R. Girlanda *et. al.* (Kluwer Academic, Amsterdam, 1989), p. 51.
[11] J. Emsley, *The Elements* (Oxford University Press, Oxford, 1991).
[12] K. Itoh, W. L. Hansen, E. E. Haller, J. W. Farmer, V. I. Ozhogin, A. Rudnev, and A. Tikhomirov, J. Mater. Res. **8**, 1341 (1993).
[13] V. F. Agekyan, V. M. Asnin, A. M. Kryukov, I. I. Markov, N. A. Rud', V. I. Stepanov, and A. B. Churilov, Sov. Phys. Solid State **31**, 2082 (1989).
[14] H. D. Fuchs, C. H. Grein, C. Thomsen, M. Cardona, W. L. Hansen, E. E. Haller, and K. Itoh, Phys. Rev. B **43**, 4835 (1991).
[15] H. D. Fuchs, P. Etchegoin, M. Cardona, K. Itoh, and E. E. Haller, Phys. Rev. Lett. **70**, 1715 (1993).
[16] G. Davies, E. C. Lightowlers, K. Itoh, W. L. Hansen, E. E. Haller, and V. Ozhogin, Semicond. Sci. Technol. **7**, 1271 (1992).
[17] P. Etchegoin, J. Weber, M. Cardona, W. L. Hansen, K. Itoh, and E. E. Haller, Solid State Commun. **83**, 843 (1992).
[18] G. Davies, J. Hartung, V. Ozhogin, K. Itoh, W. L. Hansen, and E. E. Haller, Semicond. Sci. Technol. **8**, 127 (1993).
[19] M. Cardona, *Modulation Spectroscopy*, Suppl. 11 of Solid State Physics, edited by F. Seitz, D. Turnbull, and H. Ehrenreich (Academic, New York, 1969).
[20] T. P. McLean and R. Loudon, J. Phys. Chem. Solids **13**, 1 (1960).
[21] N. O. Lipari and A. Baldereschi, Phys. Rev. B **3**, 2497 (1971).
[22] E. O. Kane, Phys. Rev. B **11**, 3850 (1975).
[23] J. R. De Laeter, K. G. Heumann, and K. J. R. Rosman, J. Phys. Chem. Ref. Data **20**, 1327 (1991). See column 9 on p. 1331.
[24] Syton HT-50, Monsanto LTD, distributed by REMET Chemical Corp., Bleachery Place, Chadwick, NY 13319.
[25] A. Gilgore, P. J. Stoller, and A. Fowler, Rev. Sci. Instrum. **38**, 1535 (1967).
[26] R. G. Alonso, C. Parks, A. K. Ramdas, H. Luo, N. Samarth, J. K. Furdyna, and L. R. Ram-Mohan, Phys. Rev. B **45**, 1181 (1992).
[27] Janis "SuperTran," Janis Reasearch, Inc., P.O. Box 696, 2 Jewel Ave., Wilmington, MA 01887-0896.
[28] R. C. Buschert, A. E. Merlini, S. Pace, S. Rodriguez, and M. H. Grimsditch, Phys. Rev. B **38**, 5219 (1988).
[29] D. E. Aspnes, *Handbook on Semiconductors*, edited by T. S. Moss (North-Holland, New York, 1980), Vol. 2, p. 109.
[30] A. Frova, G. A. Thomas, R. E. Miller, and E. O. Kane, Phys. Rev. Lett. **34**, 1572 (1975).
[31] M. Cardona, P. Etchegoin, H. D. Fuchs, and P. Molinàs-Mata (unpublished).
[32] Davies *et al.* in Ref. 16 drew attention to the significance of this volume term. Note that their numerical estimate must be corrected by a factor of 3 since $\Delta V/V \approx 3\Delta a/a$, where a is the lattice parameter.
[33] U. Schmid, N. E. Christensen, and M. Cardona, Solid State Commun. **75**, 39 (1990).
[34] M. Chandrasekhar and F. H. Pollak, Phys. Rev. B **15**, 2127 (1977).